Parametric Analysis of a Light Aircraft Wing Rib Utilizing Abaqus, NESSUS, and Python

Submitted by:

Adam Michalak
FEGN 528 – FEA for Advanced Design Applications

May 12, 2021

Executive Summary

This design optimization study of a light aircraft wing rib aimed to identify the material thickness and material type which would create an optimized wing rib. Three types of common aerospace grade Aluminum Alloys were studied at varying material thicknesses. It was found that a rib constructed to a thickness of 2 mm and made out of Aluminum 6061 would provide a viable option in a light aircraft's wing. If the Rib design of 2 mm is chosen to move past this preliminary design stage, a more in-depth analysis of the rib with the wing assembly should be conducted since only a distributed pressure force was applied to the bottom surface of the rib in this design study.

Introduction

The most vital part of any aircraft is the wing and its structural components. Inside a cantilevered wing one will find a spar and a set of ribs as the main structural components. The spar resembles an I-beam and typically runs from the fuselage to the wing tip. The ribs are located throughout the wing and they are what help create the shape of the wing and are responsible for transferring the load the wing experiences to the spar. An aircraft wing is typically constructed of an aluminum alloy. In this study, the design of a typical light aircraft wing's rib was modeled in SIMULIA's Abaqus. The model studied a single wing rib with varying material depth (thickness) and three types of Aluminum Alloys which are: Al 7075, Al 6061, Al 2024. The plane's wing was loaded with a pressure force under its maximum load that it could experience in extreme flight conditions.

The purpose of this study was to optimize the wing's rib structure with material type and depth of material to create the lightest and strongest structural wing rib.

Methods

The aircraft wing rib was modeled in SIMULIA's 2019 Abaqus CAE software. The Abaqus file was titled 'WingRib.cae' with the specific part being named 'Rib'. The materials that were used to perform an analysis on this part were Aluminum 6061, Aluminum 7055, and Aluminum 2024. Additional information can be found regarding the materials in the appendix of this report. The Rib resembled the shape of a wing and is similar in size of a light civilian aircraft such as a Cessna 172. In Figure 1 below, the geometry of the Rib can be viewed. Although Abaqus is dimensionless, the units used throughout the sketch are in millimeters. The Rib had a length of 420 mm and a height of 59.9 mm.

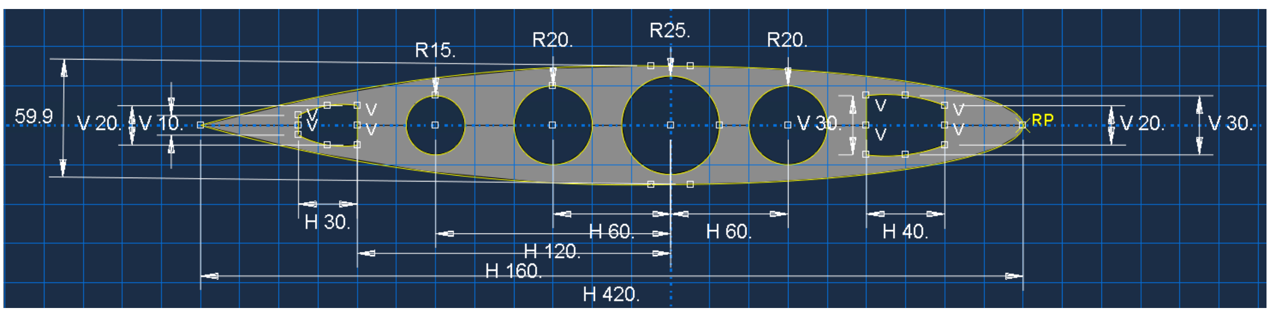

Figure 1. Rib Sketch and Geometry

The Rib's depth along the Z-axis was parametrically studied along with the type of material under the same load. The Rib's depth was changed in Abaqus with a Python script titled 'update_rib.py'. Figure 2 below displays the depth of the Rib's geometry along the Z-axis. The depth of the part varied in the optimization study from 2 mm to 6 mm.

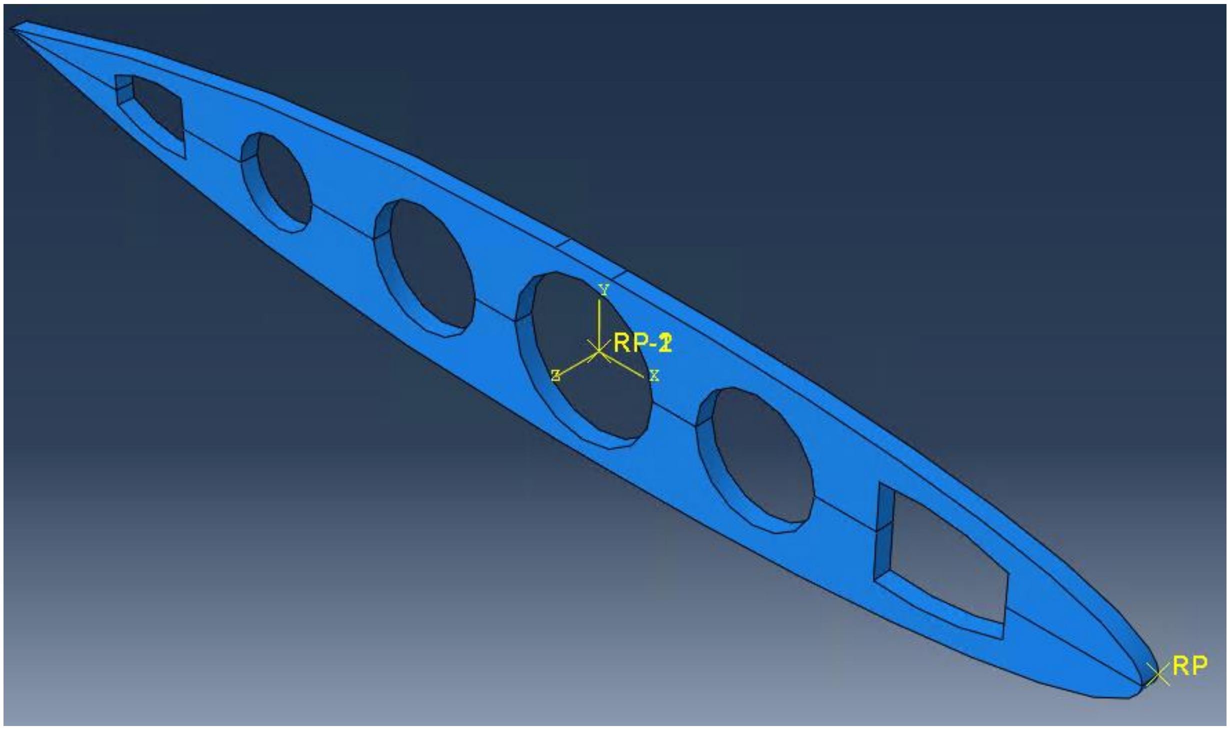

Figure 2. Rib Part Extruded along the Z-axis to a Depth of 6 mm

The Rib was optimized using NESSUS 9.95 and two Python scripts that worked together with SIMULIA's Abaqus to run simulations and extract a peak von Mises stress value that was seen in the Rib. The type of Deterministic Analysis performed by NESSUS is called a Three Level Full Factorial Analysis which analyzes the various parameters and their properties at varying part depth. The NESSUS file used to perform the deterministic analysis was titled 'WingRib.dat' and the two Python scripts that were used are titled 'update_rib.py' and 'extract_s.py'.

Table 1. Three Level Full Factorial Analysis of Rib part, set up in NESSUS.

Trial Number	Yield Strength (MPa)	Depth (mm)
0 (Mean values)	71050	4
1	69000	2
2	70000	2
3	73100	2
4	69000	4
5	70000	4
6	73100	4
7	69000	6
8	70000	6
9	73100	6

The yield strength is associated to each material type which can be found in the material properties which is in the appendix of this report. For example, Al 2024-T3 had a Yield Strength of 73.1 GPa and it was analyzed at three different material depths, 2 mm, 4 mm, and 6 mm. Three dimensions were studied for each material in order to identify if a non-linear relationship existed amongst the peak von Mises stress and the extrusion depth of the Rib.

The Boundary Conditions of the model were set using a Multi-Point Constraint also referred to as a MPC constraint. The MPC constraint was a beam type constraint as seen in Figure 3 below. The constraint was applied to the origin of the part (0,0,0) and then extended to the inner surface of the circle on the Rib. The Boundary condition can also be seen below in Figure 4. The Boundary Condition constrained Reference Point one, which is what binds the MPC to the origin, in the U_X, U_Y, and U_Z directions. Rotations were constrained in the U_{RX}, U_{RY}, U_{Rz} directions. This fully bound rigid constraint represents the Rib transferring the load to the spar which runs from fuselage to wing tip and is the primary structural component.

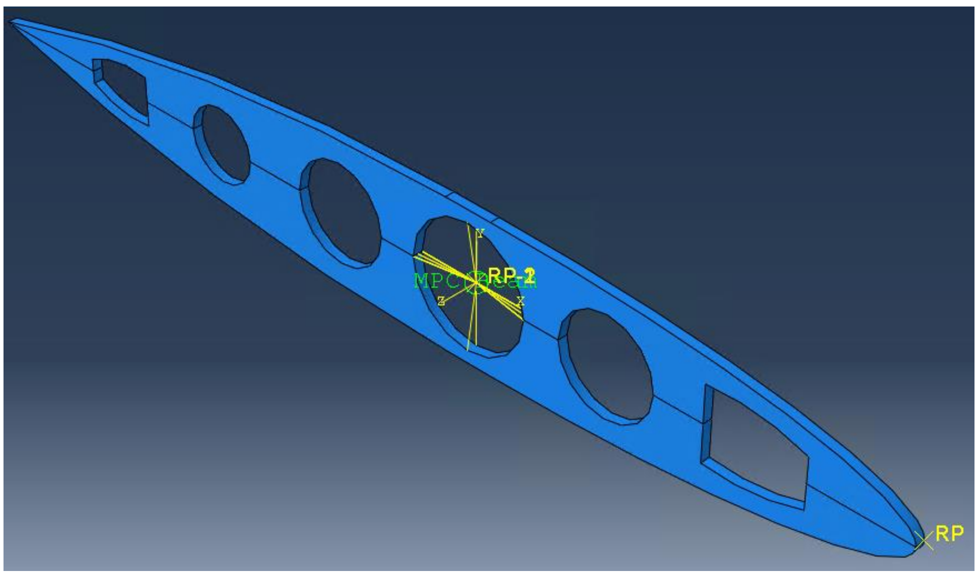

Figure 3. Multi-Point Constraint on the Rib part

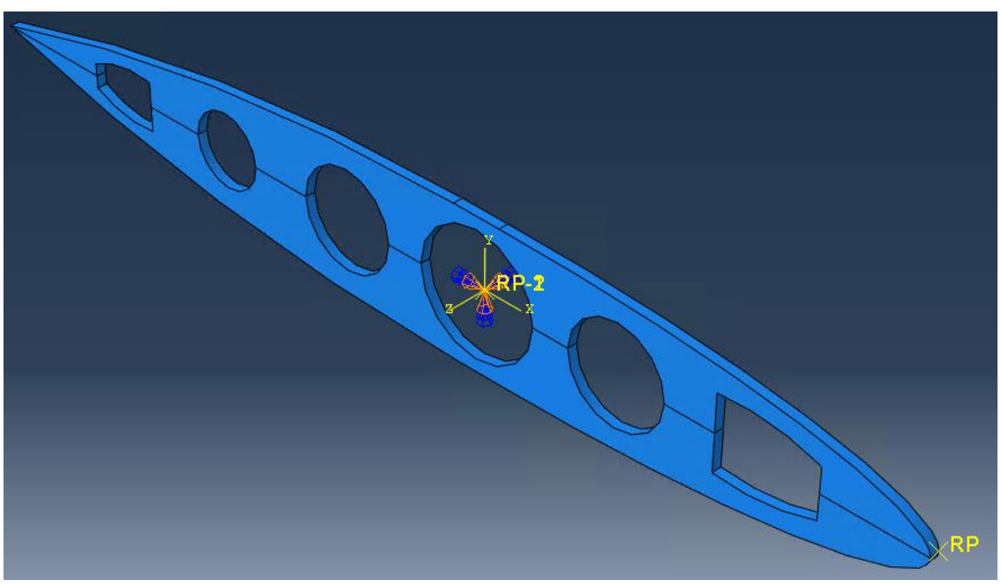

Figure 4. Boundary Condition on the Rib part

With the Boundary Conditions and MPC set up as noted above, a static pressure load of approximately 1225.8 Newtons was applied to the bottom surface of the Rib part as seen in Figure 5. The load used in the analysis is an approximation of a light aircraft such as a Cessna 172 at a Max Takeoff Weight of 1,111 kg under extreme conditions (Cessna). Details of the specific load and how it was calculated will be in the equations below. The load applied is a simplified version of a load a wing would actually receive, however, for purposes of this study the load was applied accordingly.

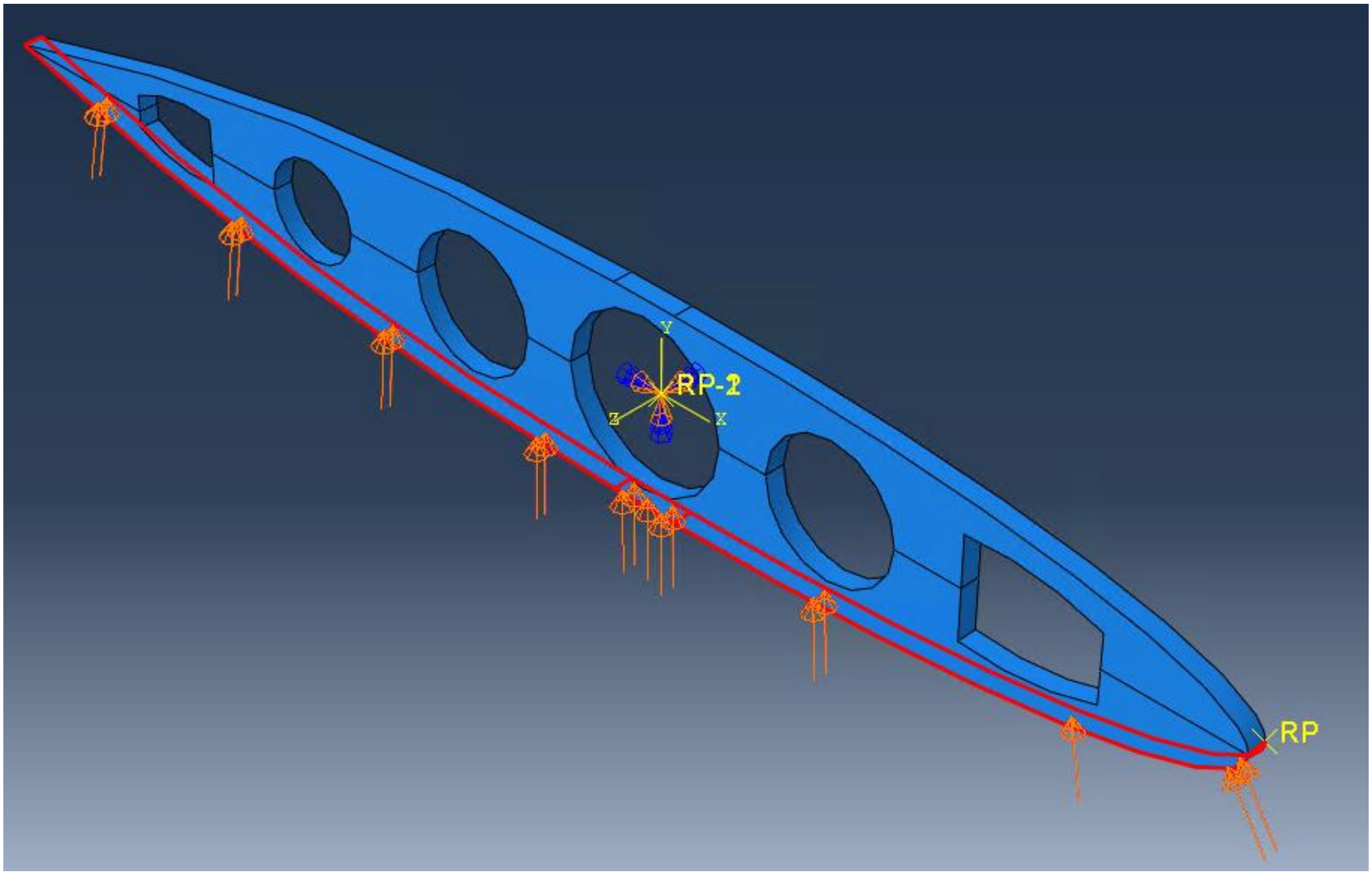

Figure 5. Pressure Load on Rib part

$$1000\ kg * 9.8065\ N = 9806.5\ N \qquad (1)$$

$$9806.5\ N * \left(2.5g_{Extreme\ Load\ Conditions} + 1g_{Factor\ Of\ Safety}\right) = 34322.75\ N \qquad (2)$$

$$\frac{34322.75\ N}{2\ wings} = \frac{17161.375\ N}{wing} \qquad (3)$$

$$\frac{17161.375\ N}{14\ Ribs} = 1225.8125\ N\ per\ Rib \qquad (4)$$

The equations above represent a light aircraft of 1000 kg mass being converted into Newtons (1). The mass is then multiplied by a force equivalent to extreme loading conditions and a 1g factor of safety (2). The term ‘g’ represents load factor equivalent to the mass of the aircraft. To be clear, the load factor ‘g’, is representative of an aircraft that is in flight at a constant speed and altitude. Any additional ‘g’ forces would make this number rise above 1, this for example could be increased acceleration, a banked turn, heads winds, or a wind gust. Including the new found load for the wings accounting for the factor of safety, the load per wing was determined (3). The load was then divided amongst ribs for the analysis to be completed of a single rib (4).

For the mesh of the model a C3D8R element type was used to mesh all three geometries of the Rib part. Each geometry type consisted of 403 elements and 1060 nodes. The mesh's for all three geometries can be seen below in Figures 6, 7, and 8 with their respective depths in the figure description.

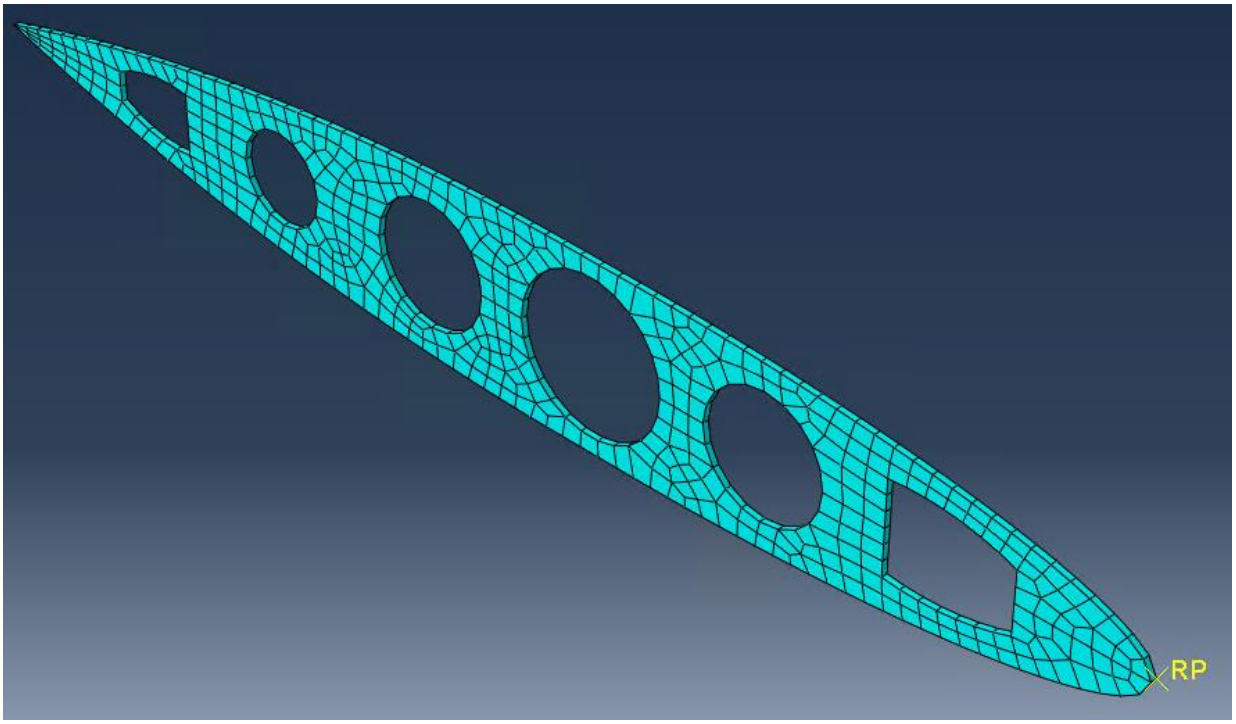

Figure 6. 2 mm Depth, 403 C3D8R Elements and 1060 nodes

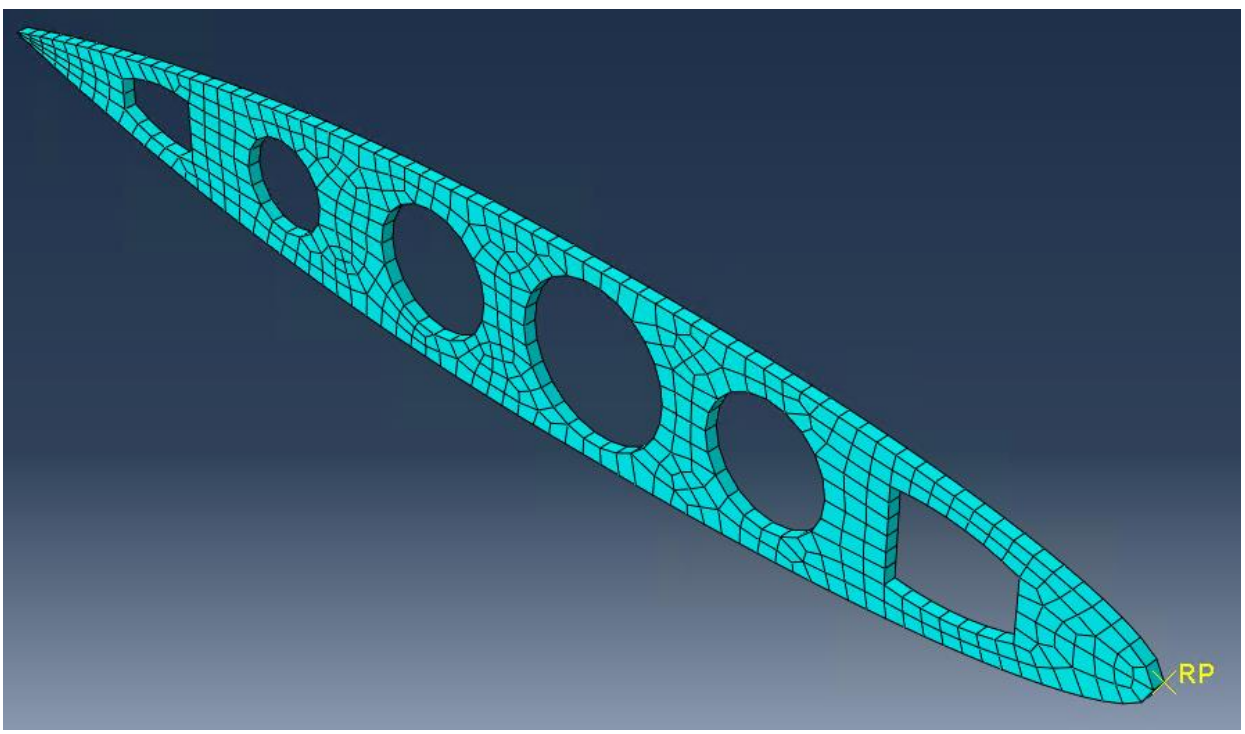

Figure 7. 4 mm Depth, 403 C3D8R Elements and 1060 nodes

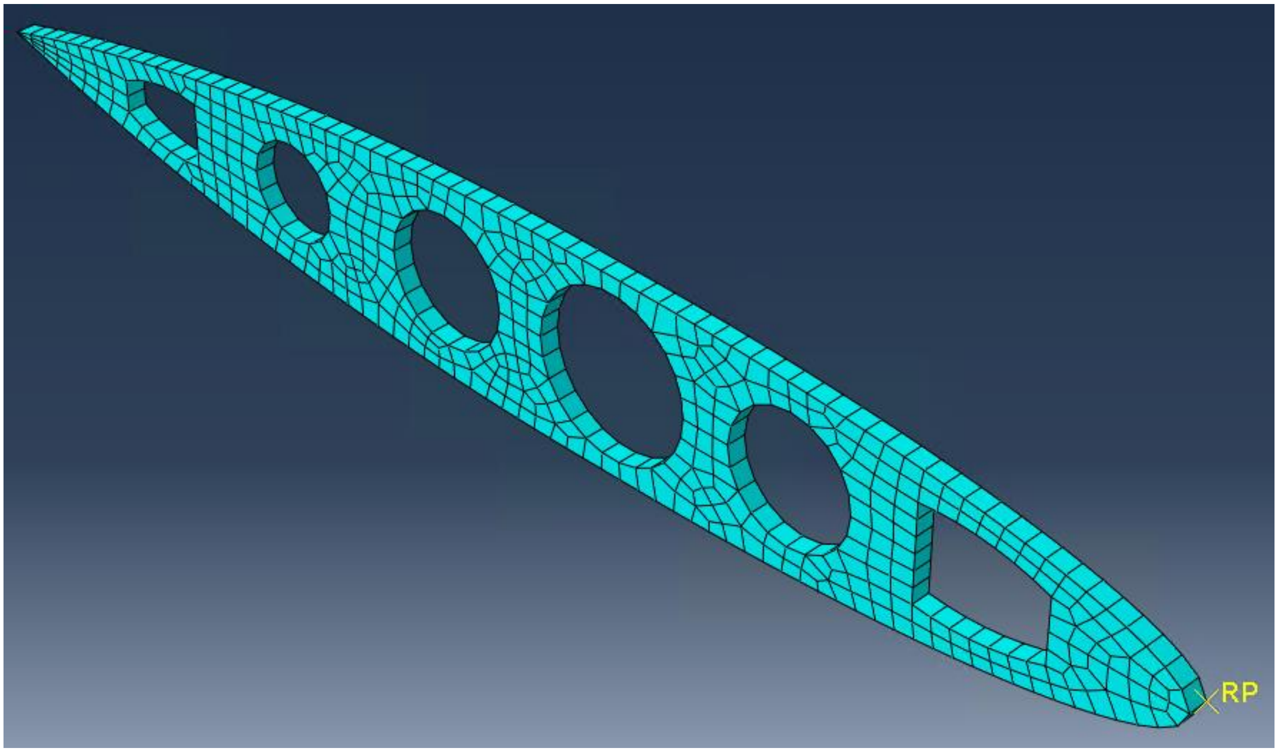

Figure 8. 6 mm Depth, 403 C3D8R Elements and 1060 nodes

For the purposes of this parametric study mesh convergence was not performed. However, in a more in depth analysis after a preliminary design study, mesh convergence should be considered. It should be noted that each material had the same three meshes respective to their unique depth. For example, the 6 mm depth Rib part mesh was shared by Al 7075, Al 6061, and Al 2024.

With the information mentioned above, the parametric study was able to be conducted in a four part process with Python as an input script, NESSUS interacting with Python conducting the separate trials, Abaqus to carry out the analysis, and finally with Python extracting the result and creating a 's_value.txt' file. The NESSUS file which was used for the study is titled 'WingRib.dat' and the two Python scripts used are titled 'update_rib.py' and 'extract_s.py'. The NESSUS file operates using a problem statement which then is linked to the Python script 'update_rib.py' as seen in Figure 9 and Figure 10. NESSUS would then supply Python the material type, specifically each material's Young's Modulus and the depth of the material to be ran through the 'update_rib.py' script. The 'extract_s.py' script would then extract the peak von Mises stress seen in the Rib part for each specific trial in NESSUS and print it to the Abaqus replay file titled 'abaqus.rpy'. The NESSUS deterministic analysis set up can be seen in Figure 11 below.

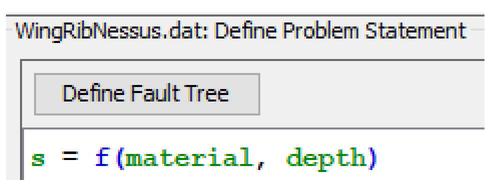

Figure 9. NESSUS problem statement

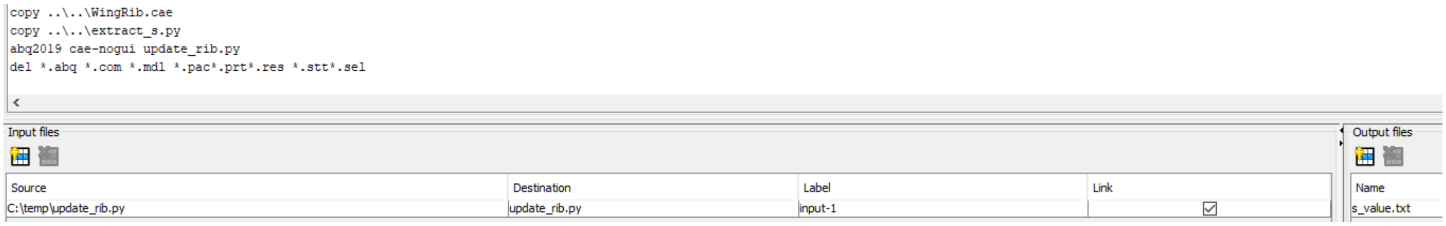

Figure 10. NESSUS Execution Command with Input and Output files

#	Comment	material	depth
0	Mean value	71050.0	4.0
1		69000.0	2.0
2		70000.0	2.0
3		73100.0	2.0
4		69000.0	4.0
5		70000.0	4.0
6		73100.0	4.0
7		69000.0	6.0
8		70000.0	6.0
9		73100.0	6.0

Figure 11. NESSUS set up for three aluminum alloys and their depth

Results

The results of the optimization study showed that the minimum depth studied for all three materials was strong enough to endure the calculated load applied to the Rib. Details of the results from the optimization study can be found in Table 2 below.

Table 2. Materials and their respective peak von Mises stress experienced with varying material depth

	Material Depth 2 mm	Material Depth 4 mm	Material Depth 6 mm
Aluminum 7075	68.16 GPa	68.16 GPa	68.16 GPa
Aluminum 6061	68.16 GPa	68.16 GPa	68.16 GPa
Aluminum 2024	68.16 GPa	68.16 GPa	68.16 GPa

The maximum peak von Mises stress was found at Element 122, Node 168, for each of the iterations of the Rib part. This maximum von Mises stress can be seen in the geometry below in Figure 12. The results appear to be accurate due to the linear application of the pressure distributed to the bottom surface of the Rib geometry. The results show a constant relationship with each other and the depth parameter does not experience non-linearity in this analysis. It should be noted that Aluminum 6061 was about 1 GPa from failing in this study. However, a large factor of safety was already taken into account in the load application.

A mesh analysis was not performed in this study as it was not the primary focus. If the design was to move forward past a preliminary stage it should be studied in more depth and a mesh analysis should be performed.

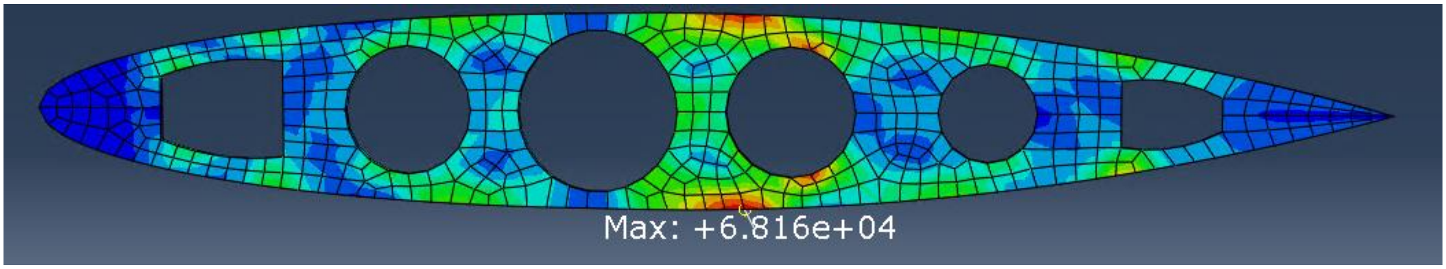

Figure 12. Max von Mises Stress on Rib geometry at E:122 N:168

As seen in the appendix, the material properties for Aluminum 6061-T4 show that is has the lowest density amongst the alloys studied for this analysis. In Table 3 below, the mass of each rib at 2 mm in depth (material thickness) will be presented. The volume of the 2 mm Rib part was 23455.4 mm^3.

Table 3. 2 mm Rib part and material type with their associated density and mass

	Density (g/cc)	Mass (g)
Aluminum 7075	2.86	67.1
Aluminum 6061	2.70	63.3
Aluminum 2024	2.78	65.2

In conclusion, the alloy which would best fit the application would be Aluminum 6061 due to its low mass and its Young's Modulus being above the maximum von Mises stress observed.

Discussion

The purpose of the study was to optimize the material type and depth of material (thickness) for a light aircraft's wing rib. By analyzing multiple configurations of geometries and material types an optimized design with a clear choice was the desired outcome. For example, the ideal design would be an aluminum alloy which could withstand the load at the smallest depth possible. However, what the results yielded is that all of the materials and their respective geometries could withstand the load. Leaving it up to density, fatigue resistance, and corrosion properties to be a potential deciding factor. For purposes of this study, only density was looked at as the determining factor since all three alloy choices are common amongst aircraft. In addition, if further analysis would need to be performed and if this design was chosen, a mesh convergence study would be recommended in order to ensure accuracy of the analysis.

In reflection, the load application could have been applied differently and incorporate other parts of the wing to get the true optimization of the wing's rib component. With that being said the results have highlighted how integral of a role each component of a wing's structure is. As mentioned in the method's section, a wing has multiple structural components such as the spar which helps the wing with bending moments, the stringers which help dampen the wing and prevent torsion, and the rib which helps distribute the load to the spar and stringers. The load which was applied to the Rib and the factor of safety that is assumed by the problem is an extreme scenario for the rib and under normal flying conditions the Rib would experience approximately 350 N of load opposed to the 1225 N applied to the Rib in this analysis. The author of this report recognizes that for a more thorough study of the Rib different loads should be applied with additional wing components to understand if the Rib can withstand shear stresses and torsion within the same failure tolerance of the spar and stringers.

In terms of verification and validation, this optimization study only provided a preliminary level of verification. Further steps would be to model the Rib with a larger wing assembly that includes a spar and stringers. This wing assembly should also experience in-depth analysis to test vibration, shear stresses, bending, buckling, and torsion. The wing being fully fixed to the fuselage and the rest of the wing being cantilevered out to the wing tip with the parts in the wing's assembly constrained to each other accordingly. This scenario would create a solid foundation for a more detailed analysis. In terms of validation, load testing can be performed on the wing and rib structure such as in Figure 13 below. The most validating experiment would ultimately be a flight test with proper instrumentation onboard and to perform a series of maneuvers that can be compared to their empirical values versus experimental values.

Figure 13. Boom Supersonic's Wing undergoing Load Testing (source: Boom Supersonic)

Overall, the material selected in this optimization study proved to be a common choice throughout the aerospace industry for light aircraft. For example, Aluminum 7075 is known for its durability and its excellent fatigue resistance which is why it is common in military aircraft; Aluminum 6061 is common in light aircraft's fuselages and wings; Arguably the most common alloy in aerospace is Aluminum 2024 due to its high tensile strength (Smye 2018).The material depth of the selected Rib also resembles an academic study of aircraft ribs where the depth was 1 mm (Dharmendra et. Al 2020). The reassuring aspect of this optimization study is that when compared to the work of a much more in-depth design study of an Aircraft's wing rib, "*Design and Analysis of an Aircraft Wing Rib for Different Configurations" by Dharmendra et. Al*, the alloy types and optimized rib thickness of 2mm were comparable. Overall with a fair level of confidence the author of this report believes a rib constructed to a thickness of 2 mm and made out of Aluminum 6061 would provide a viable option in a light aircraft's wing development.

References

1. Smye, B. (2018, October 04). Aluminum Alloys for Aerospace. Retrieved from https://www.aerospacemanufacturinganddesign.com/article/aluminum-alloys-for-aerospace/
2. Smith, M 2009, ABAQUS/Standard User's Manual, Version 6.9. Dassault Systèmes Simulia Corp, Providence
3. Dharmendra, P., Chaithanya, K., Sameera, A., Kavathiya, K., & Monika, K. (2020). DESIGN AND ANALYSIS OF AN AIRCRAFT WING RIB FOR DIFFERENT CONFIGURATIONS. *International Research Journal of Engineering and Technology (IRJET), 07*(06), June 2020, 180-192.
4. ASM Engineered Materials Reference Book, Second Edition, Michael Bauccio, Ed. ASM International, Materials Park, OH, 1994.
5. Cessna Skyhawk. (n.d.). Retrieved May 11, 2021, from https://cessna.txtav.com/en/piston/cessna-skyhawk

Appendix

Material	Young's Modulus (GPa)	Poisson's Ratio	Density (g/cc)
Aluminum 7075	70	0.33	2.86
Aluminum 6061	69	0.33	2.70
Aluminum 2024	73.1	0.33	2.78

Source: ASM Engineered Materials Reference Book (matweb.com)

Credit

The author of this report would like to thank Dr. Petrella for helping develop the 'extract_s.py' script and the general guidance in this report.